

# Flow Control with Intermittent Disturbance for the Laminar Separation Bubble on a NACA633-421 Airfoil

SIPKADUWA MADUWA GURUGE Supun Induwara Perera,  
LI Linkai\*, WANG Shilong

College of Aerospace Engineering, Nanjing University of Aeronautics and Astronautics, Nanjing 210016, P. R. China

(Received 18 January 2024; revised 13 July 2024; accepted 5 August 2024)

**Abstract:** This study investigates the aerodynamic performance of the NACA 633-421 airfoil and the effectiveness and feasibility of intermittent disturbance flow control methods on laminar separation bubbles (LSBs). It is found that the average velocity and influence range of the synthetic jet actuator increase with the increasing of driving frequency and driving amplitude. LSB occurs at  $Re=1.0\times 10^5$ , and ruptures at  $\alpha=6^\circ$ . But with intermittent disturbance control, the stall angle of attack (AoA) increases while significantly reducing drag. Research shows that although certain disturbance cannot fully recover from LSB stall, decreasing driving amplitude partially restores wing aerodynamic performance, more effectively than increasing driving amplitude.

**Key words:** laminar separation bubble; intermittent disturbance control; driving frequency; driving amplitude; synthetic jet actuator

**CLC number:** V1

**Document code:** A

**Article ID:** 1005-1120(2024)S-0001-12

## 0 Introduction

The behavior of fluid flow on surfaces is crucial to understanding fluid dynamics. The laminar separation bubble is a particularly fascinating phenomenon in this sector that has a major impact on the effectiveness and performance of numerous engineering systems. A laminar boundary layer separating away an object's surface and forming a turbulent flow area that reattaches further downstream is known as a laminar separation bubble (LSB). The LSB develops when there is a pressure drop along an object's surface, causing the flow over the object to transition from laminar to turbulent. This phenomenon usually occurs during low Reynolds numbers. In more details, for example, when it comes to an airfoil or a flat plate, the boundary layer is initially laminar close to the leading edge. Adverse pressure gradients can be produced by the fluid flowing over the surface due to variations in surface cur-

vature or outside factors. This is the area where the laminar boundary layer slows down due to an increase in pressure in the flow direction. The laminar boundary layer separates from the surface if the adverse pressure gradient is sufficiently large. When this happens, the fluid flows backward in relation to the free stream, creating a bubble of recirculating flow. Turbulence may replace the initially laminar flow inside the separation bubble if it becomes unstable. Various instabilities inside the separated shear layer are responsible for this transition. Because of its increased momentum close to the surface, the turbulent boundary layer can overcome the adverse pressure gradient and reattach to the surface downstream of the separation point. Designing efficient and effective aerodynamic systems, like as wings, propellers, and turbines, requires an understanding of the behavior of LSBs. Also, these bubbles are frequently seen on leading edges of thin airfoils, gas turbine blades, and low Reynolds number micro-

\*Corresponding author, E-mail address: linkaili@nuaa.edu.cn.

**How to cite this article:** SIPKADUWA MADUWA GURUGE Supun Induwara Perera, LI Linkai, WANG Shilong. Flow control with intermittent disturbance for the laminar separation bubble on a NACA633-421 airfoil[J]. Transactions of Nanjing University of Aeronautics and Astronautics, 2024, 41(S): 1-12.

<http://dx.doi.org/10.16356/j.1005-1120.2024.S.001>

aero-vehicle wings. If not managed properly LSBs can increase drag, decrease lift, induce flow instabilities (unsteady and unpredictable behavior) and many more. The behavior of LSBs is studied by scientists and engineers using a range of approaches, such as computational fluid dynamics (CFD) simulations and wind tunnel tests, to improve the design of aerodynamic systems. For aerodynamic devices to be designed effectively, it is crucial to comprehend the science of the laminar separation bubble and its potential controls<sup>[1-9]</sup>. A LSB is illustrated in Fig.1.

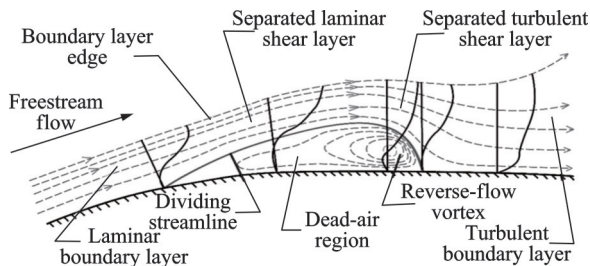


Fig.1 Schematic of a LSB<sup>[10]</sup>

## 1 Methodology

A 2D NACA633-421 laminar airfoil model was created specifically for this experiment. According to the NACA number, the maximum camber was 6% of the chord, the maximum camber was located 33% of the chord from the leading edge and the maximum thickness was 42% of the chord. In this particular experimental model, as shown in Fig.2, the chord length was  $c=250$  mm and the span length was  $L=550$  mm. At the half-span of the airfoil surface, 55 pressure taps were also installed. The diameter of each pressure tap was 0.6 mm. On the upper surface of the airfoil model, six synthetic jet actuators were equally included with identical span-wise spacing,  $d=80$  mm. These actuators were located at 30% of the chord from the leading edge. Each actuator featured two splay slots with dimensions of 15 mm in length, 1 mm in width, and a  $15^\circ$  splay angle. As shown in the Fig.2, a small loudspeaker functioned as the actuator. The coil moved up and down when the driving signal was applied to the actuator, with the help of an electric current. The membrane then moved up

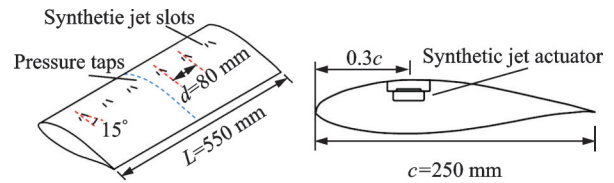


Fig.2 Experimental model (parameters & synthetic jet actuators)

and down in order to create two vortexes at the slots' exit.

The wind tunnel used for the present study was a 0.8 m suctional closed wind tunnel (Fig.3). The size of the test section was 0.8 m  $\times$  0.8 m, the wind speed ranged from 5m/s to 40 m/s, and the turbulence was about 1%. The main experiment was conducted to investigate the aerodynamic performance of the NACA 633-421 airfoil at low Reynolds numbers and LSB flow control with an intermittent disturbance on the airfoil. Studies of the behavior of objects or fluids in a controlled airflow environment frequently involve wind tunnel experiments. The NACA 633-421 airfoil model was placed in the middle of the wind tunnel test section. The model was connected to the six-axis force/torque balance to collect accurate forces and torque information, which was connected to the high precision rotary table to change the angle of attack. Waveform generator was connected to the power amplifier, which was connected to the synthetic jet actuators inside the model. Model's pressure taps were connected to the pressure data acquisition (DAQ) to collect accurate pressure measurements of the airfoil. To determine the proper revolutions per minute (RPM) for the required airspeeds, a pitot tube was used. Dynamic pressure could be calculated by combining the pitot pressure and static pres-

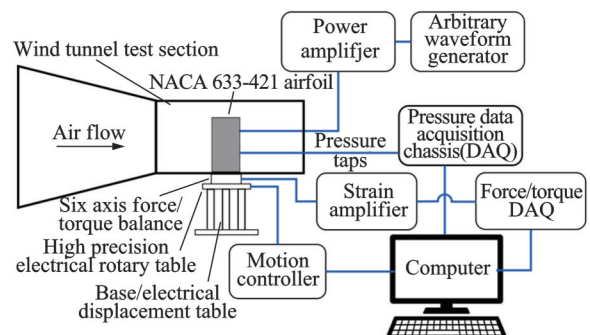


Fig.3 Experimental setup for the wind tunnel test

sure. The dynamic pressure formula can be used to determine airspeed from the dynamic pressure. For Reynolds numbers  $0.7 \times 10^5$ ,  $1.0 \times 10^5$ ,  $1.4 \times 10^5$ ,  $1.7 \times 10^5$ , the corresponding airspeeds were 4, 6, 8, 10 m/s, and the corresponding wind tunnel RPMs were 120, 185, 225, 295 r/min. Before the start of the experiment, the high precision rotary table, pressure system and the force/torque system were calibrated accordingly. The data for baselines 4, 6, 8, and 10 were gathered after the airflow was started. Following that, various synthetic jet actuator frequencies and amplitudes were utilized, as shown in Table 1, for each baseline to gather further data (for each case angle of attack from  $-6^\circ$  to  $26^\circ$ ).

**Table 1 Experiment frequencies and amplitudes**

Frequency/Hz	Amplitude/V
0.1	1
0.2	1
0.5	1,3,5
2	1,3,5
4	1,3,5
6	1,3,5

## 2 LSB Flow Control with an Intermittent Disturbance

The bursting of the LSB as it gets near the leading edge is the primary cause of the stall to occur at low angle of attacks and Reynolds numbers. The mean lift coefficient curves at various angle of attacks, with and without intermittent disturbance control, are shown in Figs.4,5. In the baseline ( $Re=1.0 \times 10^5$  without control), the stall occurred at  $\alpha=6^\circ$  but with the driving frequency 0.5 Hz and driving amplitude 1 V, the angle of stall increased to  $\alpha=18^\circ$ , which is three times higher than the baseline. For the driving frequency 6 Hz and driving amplitude 5 V, the angle of stall increased to  $\alpha=26^\circ$ , which is more than four times higher with the baseline. Additionally, Figs.6,7 show nearly the same characteristics as Fig.5. Fig.8 shows the mean lift coefficient curves for the driving frequency 0.1 Hz and driving amplitude 1 V, the angle of stall moves from  $\alpha=6^\circ$  to  $\alpha=14^\circ$ , but the mean lift coefficient moves from  $-6^\circ$  to  $14^\circ$  as an irregular increase.

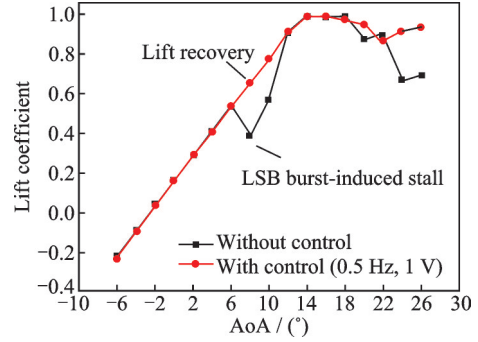


Fig.4 Lift characteristics of NACA 633-421 airfoil with control (0.5 Hz, 1 V) and without an intermittent disturbance at  $Re=1.0 \times 10^5$

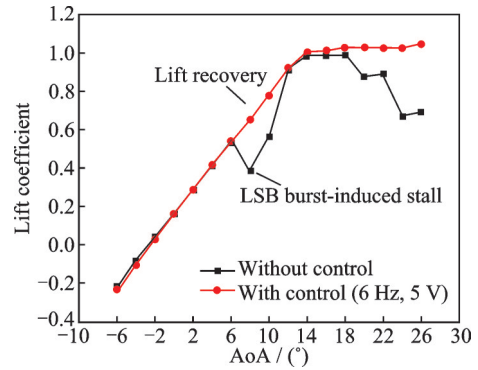


Fig.5 Lift characteristics of NACA 633-421 airfoil with control (6 Hz, 5 V) and without an intermittent disturbance at  $Re=1.0 \times 10^5$

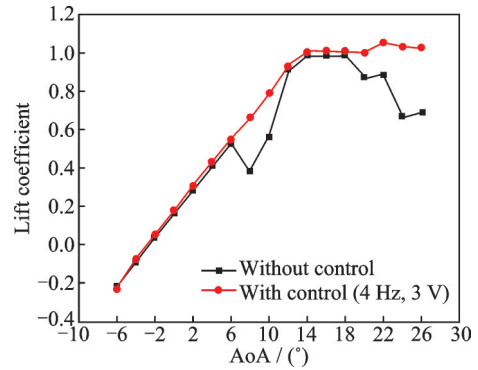


Fig.6 Lift characteristics of NACA 633-421 airfoil with control (4 Hz, 3 V) and without an intermittent disturbance at  $Re=1.0 \times 10^5$

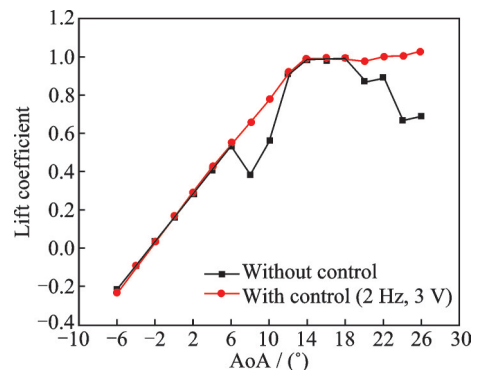


Fig.7 Lift characteristics of NACA 633-421 airfoil with control (2 Hz, 3 V) and without an intermittent disturbance at  $Re=1.0 \times 10^5$

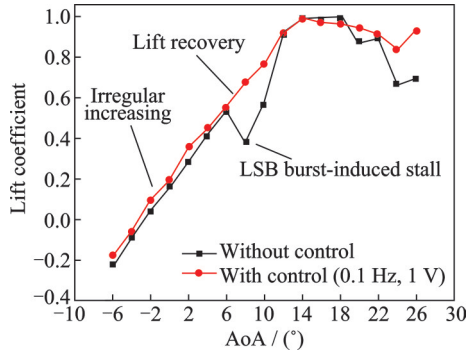


Fig.8 Lift characteristics of NACA 633-421 airfoil with control (0.1 Hz, 1 V) and without an intermittent disturbance at  $Re=1.0 \times 10^5$

At  $Re=0.7 \times 10^5$ , the mean lift coefficient curves at various angle of attacks with and without intermittent disturbance control are shown in Fig.9. In the baseline ( $Re 0.7 \times 10^5$  without control) the stall occurs at  $\alpha=0^\circ$ , but with intermittent disturbance control the stall angle extends to  $\alpha=20^\circ$  and the maximum lift coefficient increases from about 0.85 to 1.1 for the driving frequency 6 Hz and driving amplitude 1 V. In conclusion, when the intermittent disturbance control is presented and with appropriate driving frequency and driving amplitude, the existing LSB at  $Re=1.0 \times 10^5$  is maintained without bursting, which increases the stall angle of attack, thus allowing for more operational space.

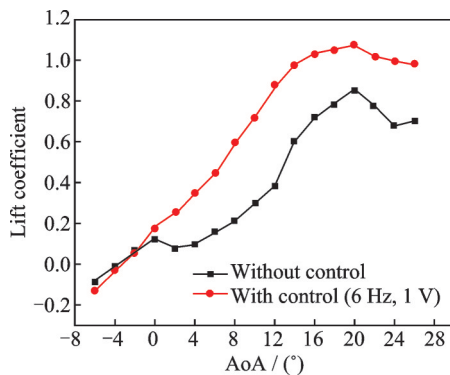


Fig.9 Lift characteristics of NACA 633-421 airfoil with control (6 Hz, 1 V) and without an intermittent disturbance at  $Re=0.7 \times 10^5$

The mean drags coefficient curves at various angle of attacks at  $Re=1.0 \times 10^5$ , with and without intermittent disturbance control, are shown in Figs.10,11. In the baseline (without control), an abrupt increase in drag can be seen after the angle of attack  $\alpha=6^\circ$ , which is due to the natural bursting

process of the LSB. This phenomenon is eliminated with the intermittent disturbance control and the mean drag coefficient curves have become smoother compared to the baseline, as shown in Figs.10,11. At  $Re=0.7 \times 10^5$ , the mean drags coefficient curves at various angle of attacks with and without intermittent disturbance control are shown in Fig.12. The mean drag coefficient curve with control of driving frequency 6 Hz and the driving amplitude 1 V is low-

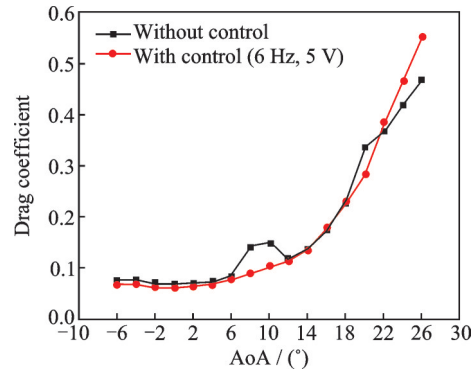


Fig.10 Drag characteristics of NACA 633-421 airfoil with control (6 Hz, 5 V) and without an intermittent disturbance at  $Re=1.0 \times 10^5$

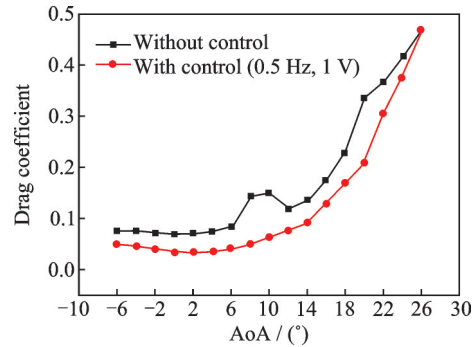


Fig.11 Drag characteristics of NACA 633-421 airfoil with control (0.5 Hz, 1 V) and without an intermittent disturbance at  $Re=1.0 \times 10^5$

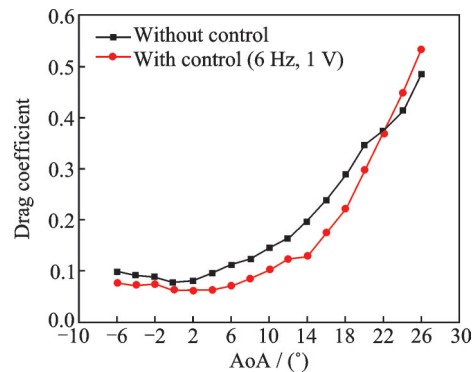


Fig.12 Drag characteristics of NACA 633-421 airfoil with control (6 Hz, 1 V) and without an intermittent disturbance at  $Re=0.7 \times 10^5$

er than the baseline (without control) until the angle of attack  $\alpha=22^\circ$ , afterwards the baseline's curve is lower. Additionally, the maximum drag coefficient is higher than the maximum drag coefficient value of the baseline, which is increased from about 0.48 to 0.54. In conclusion, with the intermittent disturbance control and with appropriate driving frequencies and driving amplitudes, the drag coefficient is relatively lower than the baseline, which enhances the performance and conserve energy as well.

## 2.1 Influence of intermittent disturbance amplitude

For some driving frequencies, the driving amplitudes needs to be lower for the lift to recover. This phenomenon is clearly shown in Fig.13. The intermittent disturbance from the synthetic jet actuator is unable to recover the lift coefficient sufficiently, but compared to the baseline, the lift coefficient curve has a higher magnitude. And compared to Fig.4, which is the same driving frequency with different driving amplitudes, the role of the driving amplitude in the synthetic jet actuator is clearly shown. Contrariwise, the mean lift coefficient curves for different driving amplitudes but with the same driving frequency are shown in Figs.14,15. For reasonably high frequencies in Figs.14,15 with comparison to Figs.4,13, all driving amplitudes are successful for stall recovery.

The lift characteristics of NACA 633-421 airfoil without and with different driving amplitudes for the same driving frequency (6 Hz) at  $Re=0.7 \times 10^5$

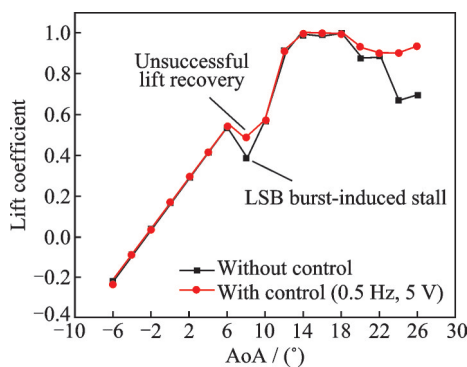


Fig.13 Lift characteristics of NACA 633-421 airfoil with control (0.5 Hz, 5 V) and without an intermittent disturbance at  $Re=1.0 \times 10^5$

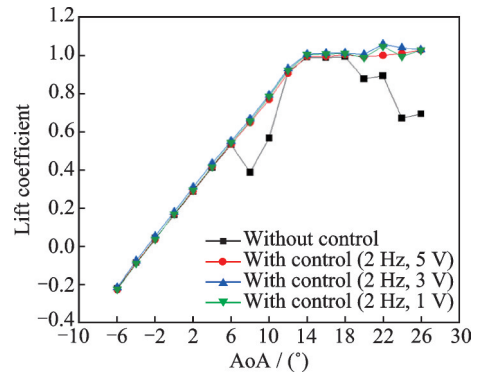


Fig.14 Lift characteristics of NACA 633-421 airfoil without and with different driving amplitudes for the same driving frequency (2 Hz) at  $Re=1.0 \times 10^5$

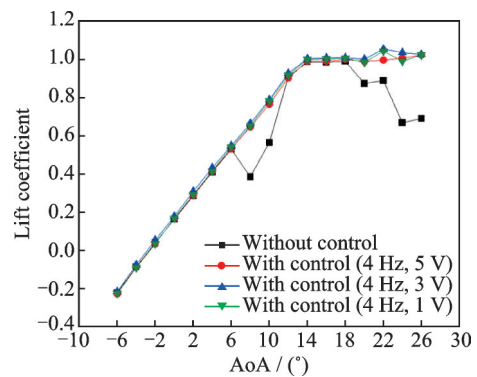


Fig.15 Lift characteristics of NACA 633-421 airfoil without and with different driving amplitudes for the same driving frequency (4 Hz) at  $Re=1.0 \times 10^5$

are shown in Fig.16, which shows that even though the amplitude is different for driving frequency 6 Hz, the mean lift coefficient curves are nearly identical for the  $Re=0.7 \times 10^5$ . Fig.17 demonstrates that the driving frequency 0.5 Hz is unable to successfully recover the lift decrease in every driving amplitude but the lift coefficient magnitude seems to be increasing.

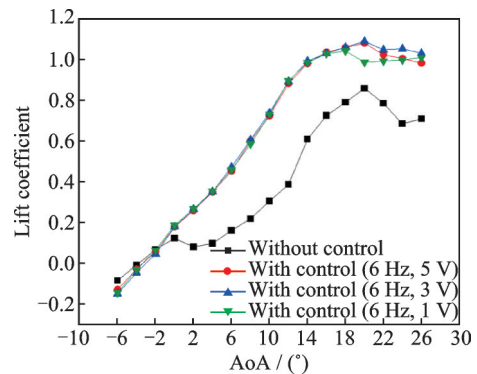


Fig.16 Lift characteristics of NACA 633-421 airfoil without and with different driving amplitudes for the same driving frequency (6 Hz) at  $Re=0.7 \times 10^5$

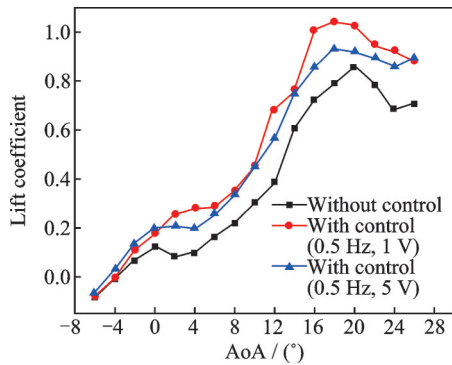


Fig.17 Lift characteristics of NACA 633-421 airfoil without and with different driving amplitudes for the same driving frequency (0.5 Hz) at  $Re=0.7 \times 10^5$

Compared with Fig.11, Fig.18 shows the drag characteristics of NACA 633-421 airfoil with and without an intermittent disturbance at  $Re=1.0 \times 10^5$ , where the driving frequencies are the same but the driving amplitude is different from that in Fig.11. For the driving amplitude 5 V, the frequency 0.5 Hz is unable to eliminate the abrupt drag coefficient increase even though the magnitude is lower than the baseline. Additionally, from Fig.19, the drag characteristics of NACA 633-421 airfoil with

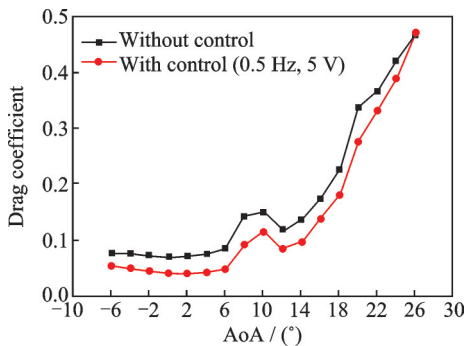


Fig.18 Drag characteristics of NACA 633-421 airfoil with control (0.5 Hz, 5 V) and without an intermittent disturbance at  $Re=1.0 \times 10^5$

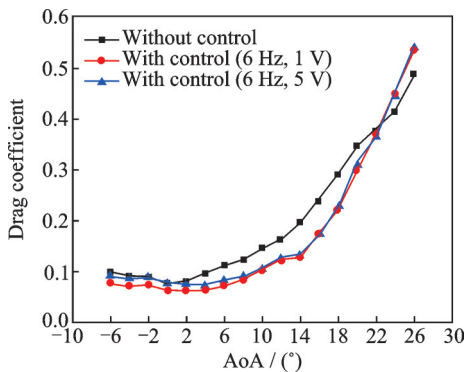


Fig.19 Drag characteristics of NACA 633-421 airfoil without and with different driving amplitudes for the same driving frequency (6 Hz) at  $Re=0.7 \times 10^5$

out and with different driving amplitudes for the same driving frequency (6 Hz) at  $Re=0.7 \times 10^5$  is featured, where the driving amplitude 1 V and 5 V mean drag coefficient curves demonstrate virtually indistinguishable characteristics.

In conclusion, with the increase of intermittent disturbance control driving amplitude, the lift coefficient magnitude and the maximum lift coefficient value are increasing, but a relatively lower amplitudes (1 V) for the intermittent disturbance control driving amplitude appears to be improving the performance, and energy consumption is also lower compared to that with 5 V. Therefore, based on these results, a conclusion can be drawn that the driving amplitude 1 V is better suited than the driving amplitude 5 V.

## 2.2 Influence of intermittent disturbance frequency

The mean lift coefficient curves for different driving frequencies (0.1, 0.2, 0.5, 2, 4, 6 Hz) but with the same driving amplitude (1 V) at  $Re=1.0 \times 10^5$ , can be seen in Fig.20, which proves that for all frequencies in the experiment, with the correct driving amplitude, the low angle of attack stall can be recovered sufficiently. Fig.21 features the lift characteristics of NACA 633-421 airfoil without and with different driving frequencies (0.5, 2, 4, 6 Hz) for the same driving amplitude (1 V) at  $Re=0.7 \times 10^5$ . Compared with different driving frequencies, 6 Hz mean lift coefficient curve surpasses other frequencies curves, as shown in Fig.22, because of the reasonable linear increase in the mean lift coefficient curve and the highest maximum lift coefficient recorded.

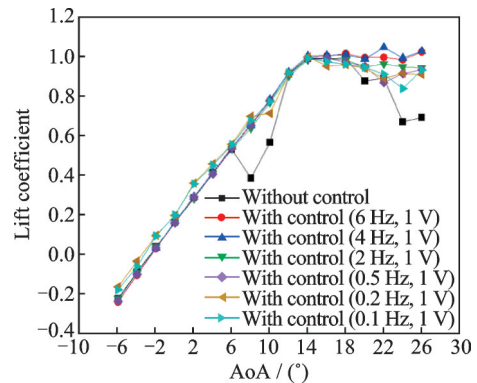


Fig.20 Lift characteristics of NACA 633-421 airfoil without and with different driving frequencies for the same driving amplitude (1 V) at  $Re=1.0 \times 10^5$

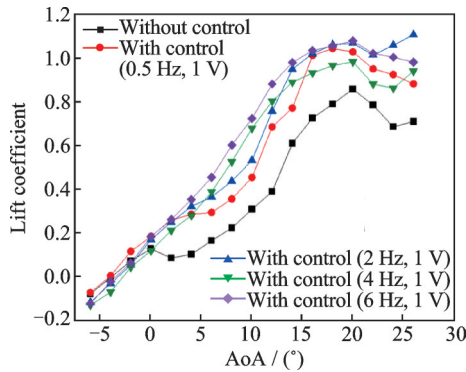


Fig.21 Lift characteristics of NACA 633-421 airfoil with-out and with different driving frequencies for the same driving amplitude (1 V) at  $Re=0.7 \times 10^5$

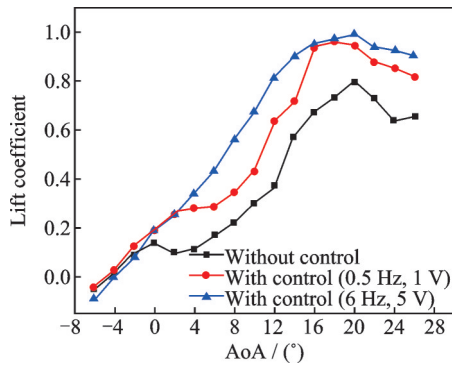


Fig.22 Lift characteristics of NACA 633-421 airfoil with-out and with control (0.5 Hz, 6 Hz) driving frequencies for 1 V driving amplitude at  $Re=0.7 \times 10^5$

As shown in Figs.10,11, for driving frequency 0.5 Hz and driving amplitude 1 V, the mean drag coefficient curve is lower than the mean drag coefficient curve for driving frequency 6 Hz and driving amplitude 5 V, which proves that with lower intermittent disturbance frequencies, the mean drag coefficient curves get lower and lower. Fig.23 shows mean drag coefficient curves at  $Re=1.0 \times 10^5$  with different driving frequencies but with the same am-

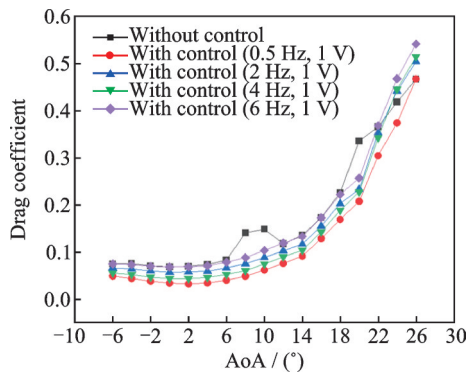


Fig.23 Drag characteristics of NACA 633-421 airfoil with-out and with different driving frequencies for the same driving amplitude (1 V) at  $Re=1.0 \times 10^5$

plitude. Fig.23 also confirms that, with lower intermittent disturbance frequencies, the mean drag coefficient curves get lower and lower.

In conclusion, with the increase of intermittent disturbance control driving frequency, the stall angle of attack increases. Therefore, for very low Reynolds numbers such as  $Re=0.7 \times 10^5$ , the intermittent disturbance control driving frequency should be higher, which turns out to be 6 Hz as the ideal frequency (irregular lift coefficient increase can be seen in lower frequencies, which can have unpredictable behavior), even though the energy consumption is higher for that driving frequency. Additionally, with the increase of intermittent disturbance control driving frequency, the drag coefficient increases, which affects the performance negatively. Hence, finding the ideal balance between these parameters is the key for intermittent disturbance control. For  $Re=1.0 \times 10^5$ , 0.5 Hz driving frequency is able to maintain the LSB without bursting. With the low driving frequency, the drag coefficient and the energy consumption is at the minimum. Therefore, based on the results, 0.5 Hz intermittent disturbance control driving frequency is the most appropriate for  $Re=1.0 \times 10^5$ .

### 2.3 Surface pressure variations

NACA 633-421 airfoil's upper and lower mean pressure coefficient curves with and without an intermittent disturbance at the angle of attack  $\alpha=10^\circ$  is featured in Figs.24, 25. The area between the upper surface curve and the lower surface curve represents the pressure difference, which directly affects the lift coefficient/lift force. From Figs.24, 25, the area in between is larger with control than that without control (baseline), thus increasing the lift coefficient/lift force significantly of the airfoil. According to Fig.26, the pressure difference between the upper and the lower surfaces in these two different control settings (6 Hz, 5 V & 0.5 Hz, 1 V), is almost the same, which means a lower intermittent disturbance frequency can be used to drive the synthetic jet actuator, thus decreasing the energy consumption of the synthetic jet actuator. In NACA 633-421 airfoil for the  $Re=1.0 \times 10^5$ , the stall occurs at an angle of attack  $\alpha=6^\circ$  with the burst of the

laminar separation. By the angle of attack  $\alpha = 8^\circ$ , the LSB is non-existent. But according to Fig.27, the laminar separation is stable and still exists at an angle of attack  $\alpha = 8^\circ$  with the intermittent disturbance. Additionally, the mean pressure coefficient curve's magnitude is much higher than that of the baseline model, which increases the pressure difference, thus increasing the lift coefficient/lift force of the airfoil.

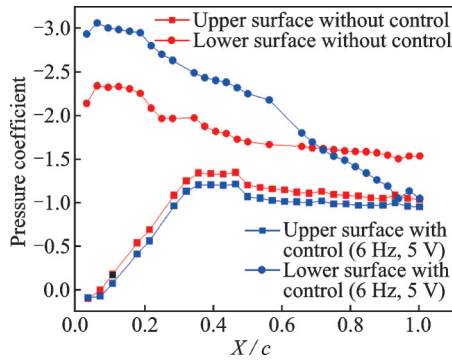


Fig.24 Pressure coefficient distribution of NACA 633-421 airfoil with control (6 Hz, 5 V) and without an intermittent disturbance at  $Re=1.0 \times 10^5$  ( $\alpha=10^\circ$ )

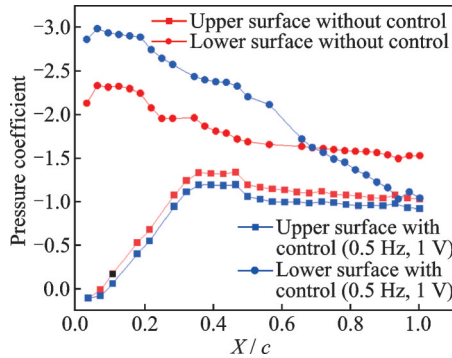


Fig.25 Pressure coefficient distribution of NACA 633-421 airfoil with control (0.5 Hz, 1 V) and without an intermittent disturbance at  $Re=1.0 \times 10^5$  ( $\alpha=10^\circ$ )

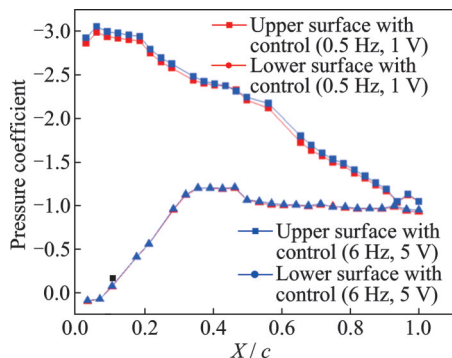


Fig.26 Pressure coefficient distribution of NACA 633-421 airfoil with intermittent disturbances (0.5 Hz, 1 V & 6 Hz, 5 V) at  $Re=1.0 \times 10^5$  ( $\alpha=10^\circ$ )

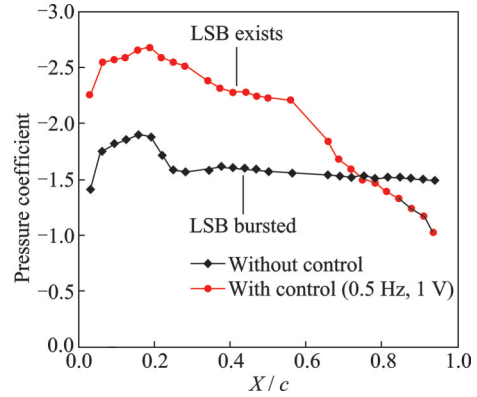


Fig.27 Pressure coefficient distribution of the upper surface at  $\alpha=8^\circ$  with control (0.5 Hz, 1 V) and without intermittent disturbance control at  $Re=1.0 \times 10^5$

Mean pressure coefficient curves with and without an intermittent disturbance control for  $Re=1.0 \times 10^5$  with different angle of attacks are shown in Figs.28, 29. After the angle of attack  $\alpha=6^\circ$  in the baseline model, the pressure decreases suddenly due to the LSB burst, which can be seen in the highlighted area in Fig.28. But after the intermittent disturbance control is being used, this scenario is eliminated, as shown in the highlighted area in Fig.29 and the LSB keeps moving towards the leading edge while maintaining the integrity.

At  $Re=0.7 \times 10^5$ , the upper and the lower mean pressure coefficient curves with and without an intermittent disturbance at the angle of attack  $\alpha=10^\circ$  is featured in Fig.30. The pressure differential, which directly affects the lift coefficient/lift force, is represented by the region between the upper surface curve and the lower surface curve. With control, the region is bigger than it is without control (base-

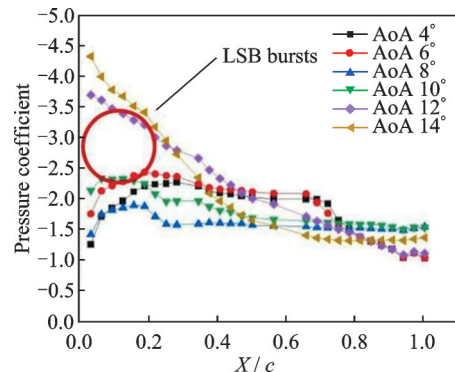


Fig.28 Upper surface pressure coefficient distributions of NACA 633-421 airfoil for different angle of attacks without an intermittent disturbance at  $Re=1.0 \times 10^5$

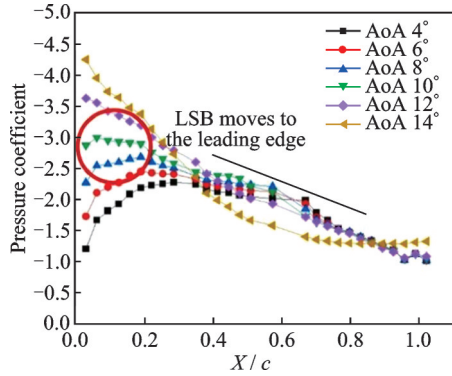


Fig.29 Upper surface pressure coefficient distributions of NACA 633-421 airfoil for different angle of attacks with an intermittent disturbance (0.5 Hz, 1 V) at  $Re=1.0 \times 10^5$

line), considerably improving the airfoil's lift coefficient and lift force. Fig.31 also shows the improvement of the upper surface mean pressure coefficient curve with control in regards with the baseline model. Also, according to Figs.32,33, the upper sur-

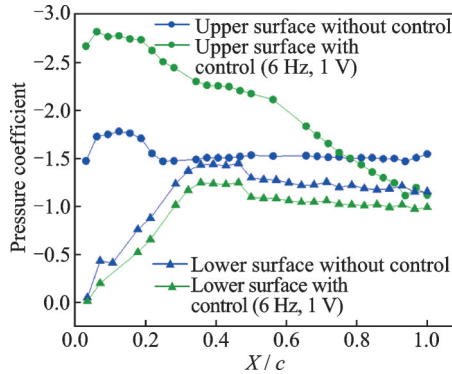


Fig.30 Pressure coefficient distribution of NACA 633-421 airfoil with control (6 Hz, 1 V) and without an intermittent disturbance at  $Re=0.7 \times 10^5$  ( $\alpha=10^\circ$ )

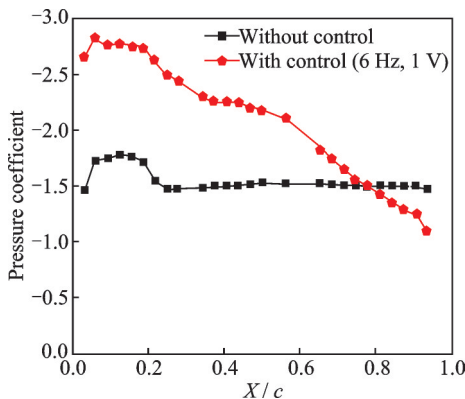


Fig.31 Pressure coefficient distribution of the upper surface at the angle of attack  $10^\circ$  with control (6 Hz, 1 V) and without intermittent disturbance control at  $Re=0.7 \times 10^5$

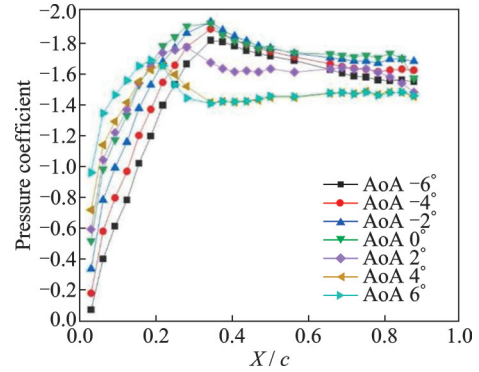


Fig.32 Upper surface pressure coefficient distributions of NACA 633-421 airfoil for different angle of attacks without an intermittent disturbance at  $Re=0.7 \times 10^5$

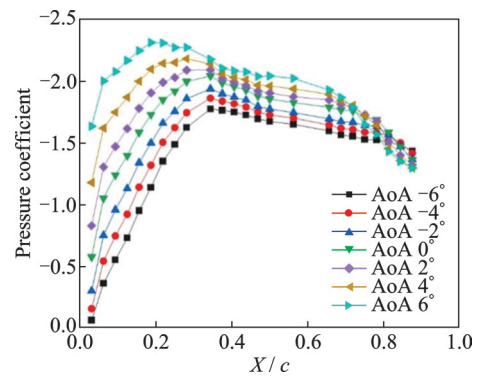


Fig.33 Upper surface pressure coefficient distributions of NACA 633-421 airfoil for different angle of attacks with an intermittent disturbance (6 Hz, 1 V) at  $Re=0.7 \times 10^5$

face mean pressure coefficient curves with an intermittent disturbance control keep increasing with the increase of angle of attack, but the upper surface mean pressure coefficient curves without an intermittent disturbance control loses pressure after the angle of attack  $\alpha=0^\circ$  due to the stall. Additionally, the maximum mean pressure coefficient has also increased with the intermittent disturbance control.

## 2.4 Energy consumption of different control parameters and efficiency

Synthetic jet actuator energy consumption can change based on a number of variables, including design, operating environment, and application. The energy consumption of a synthetic jet actuator mostly depends on the power necessary to create the pulsing motion of the fluid. The input voltage and current provided to the actuator are often used to

gauge this power usage. The energy consumption of a synthetic jet actuator can vary depending on several factors, including the design, operating conditions, and the specific application. Energy consumption of the synthetic jet actuator is calculated using Eqs. (1, 2). For each driving frequency and driving amplitude, the currents and voltages are collected using a multimeter.

$$\text{Power} = \text{Voltage} \times \text{Current} \quad (1)$$

$$\text{Energy} = \text{Power} \times \text{Time} \quad (2)$$

Although the outcomes are not very precise, Fig.34 demonstrates how energy is consumed in response to changes in the parameters of the synthetic jet actuator. Fig.34 shows that as both the driving frequency and the driving amplitude of intermittent disturbance control increase, there is an increase in energy consumption. Based on that assumption, the combination of the driving frequency 0.5 Hz and driving amplitude 1 V consumes the minimum energy, and the combination of the driving frequency 6 Hz and the driving amplitude 5 V consumes the maximum energy. Hence, for the  $Re=1.0 \times 10^5$  with the driving frequency 0.5 Hz and driving ampli-

tude 1 V can be used, which also has better performance than driving frequency 6 Hz & driving amplitude 1 V for the equivalent  $Re=10 \times 10^5$ . Additionally, for the same driving frequency with decreasing driving amplitude, the energy consumption is lower. For the same driving amplitude with decreasing driving frequency, the energy consumption is lower, which justifies selecting driving amplitude 1 V over driving amplitude 5 V. Hence, for the  $Re=0.7 \times 10^5$ , the driving frequency 6 Hz (due to the very low speed nature, relatively high frequency is needed to accomplish reasonable linear increase in the lift) and driving amplitude 1 V can be used for overall performance and energy consumption wise.

### 3 Conclusions

A NACA633-421 airfoil is chosen as the test model for this experiment. The aerodynamic performance of the NACA 633-421 airfoil at different Reynolds numbers with different angle of attacks is firstly inquired. From the investigation, it is found out that the LSB does not exist when  $Re=0.7 \times 10^5$ , but the LSB bursts when  $Re=1.0 \times 10^5$  at an angle of attack of  $\alpha=6^\circ$ . In conclusion, it may be declared that for large velocity increases and decreases, the LSB disappears and it only exists for a specific velocity range. Additionally, it is founded that with the increase of velocity, the drag coefficient decreases and the pressure differential between the upper surface and the lower surface of the airfoil gets larger and larger. The characteristics of the intermittent disturbance flow control method is also investigated. From this, it can be inferred that the outflow velocity and the jet flow rise as the driving frequency and driving amplitude of the intermittent disturbance control increase.

The LSB flow control with an intermittent disturbance is investigated as the main purpose of this experiment. It is discovered that for the  $Re=1.0 \times 10^5$ , with the intermittent disturbance control with stall angle of attack, LSB can be delayed until  $\alpha=18^\circ$  for the driving frequency 0.5 Hz and driving amplitude 1 V. For the driving frequency 6 Hz and driving amplitude 5 V, it is increased to  $\alpha=26^\circ$ . In re-

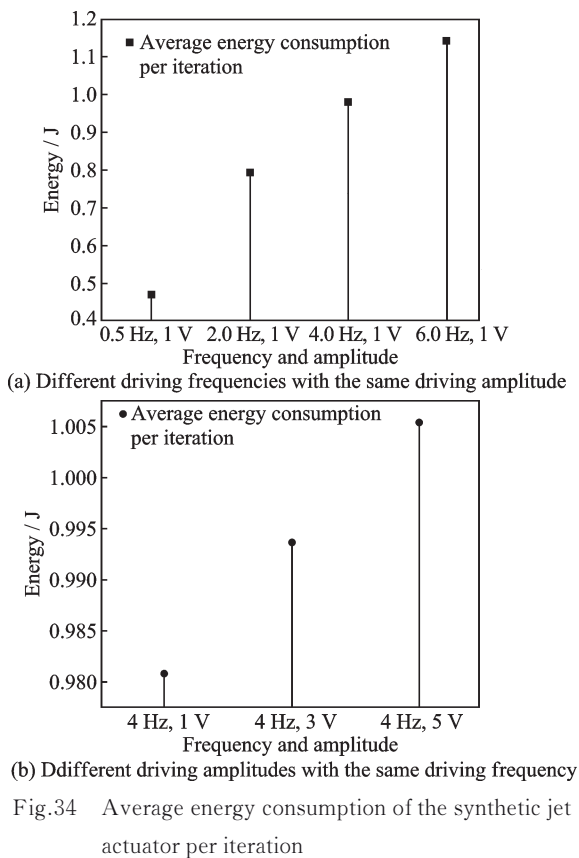


Fig.34 Average energy consumption of the synthetic jet actuator per iteration

gards with the lift coefficient and the drag coefficient, the driving frequency 6 Hz and driving amplitude 1 V have displayed nearly identical characteristics to the driving frequency 6 Hz and driving amplitude 5 V. The driving amplitude 1 V can be chosen as the better driving amplitude in regards with the energy consumption and performance. Additionally, for the comparison between the two combinations of driving frequency 0.5 Hz, driving amplitude 1 V and driving frequency 0.5 Hz, driving amplitude 5 V, it is unable to successfully recover the lift coefficient, which also supports the previous conclusion that the driving amplitude 1 V is better for every driving frequency at  $Re=1.0 \times 10^5$ . Compared with the driving frequency 6 Hz-driving amplitude 1 V, the condition of 0.5 Hz, 1 V has a low drag coefficient curve than the driving frequency 6 Hz and also manages to eliminate the abrupt drag increase at  $\alpha=6^\circ$ , which happens due to the LSB bursts, meaning the intermittent disturbance control is able to successfully maintain the LSB.

With the analysis of the mean drag coefficient curves and the upper surface mean pressure coefficient distribution curves, the laminar separation bubble does not exist when  $Re=0.7 \times 10^5$ . But with the intermittent disturbance control, the stall angle of attack is able to extend until  $\alpha=20^\circ$  from its baseline stall angle of attack  $\alpha=0^\circ$ , with the driving frequency 6 Hz and driving amplitude 1 V. This case with the 0.5 Hz driving frequency for all driving amplitudes is unable to successfully recover the lift. For the other driving frequencies 2 Hz and 4 Hz, it is able to recover the lift, but the irregular increase of the lift makes these frequencies unpredictable for use.

In conclusion;

- (1) For the intermittent disturbance control, lower driving amplitudes (1 V) is preferable;
- (2) Decreasing intermittent disturbance control frequency decreases the drag coefficient;
- (3) Increasing intermittent disturbance control frequency increases the stall angle of attack;
- (4) Increasing intermittent disturbance control amplitude increases the lift coefficient magnitude, relatively;
- (5) Increasing driving frequency and driving

amplitude increases the outflow velocity of the synthetic jet actuators.

Overall, for  $Re=1.0 \times 10^5$ , the combination of driving frequency 0.5 Hz and driving amplitude 1 V is the most suited due to the enhanced performance and the less energy consumption. For  $Re=0.7 \times 10^5$ , the combination of driving frequency 6 Hz and driving amplitude 1 V is ideal even though the LSB does not exist. For  $Re=0.7 \times 10^5$ , the intermittent disturbance control enhances performance significantly.

## References

- [1] DIWAN S S, RAMESH O N. Laminar separation bubbles: Dynamics and control[J]. *Sadhana*, 2007, 32: 103-109.
- [2] RICCI R, MONTELPARE S. A quantitative IR thermographic method to study the laminar separation bubble phenomenon[J]. *International Journal of Thermal Sciences*, 2005, 44(8): 709-719.
- [3] TOPPINGS C E, KURELEK J W, YARUSEVYCH S. Laminar separation bubble development on a finite wing[J]. *AIAA Journal*, 2021, 59(8): 2855-2867.
- [4] JAHANMIRI M. Laminar separation bubble: Its structure, dynamics and control[D]. Gothenburg, Sweden: Chalmers University of Technology, 2011: 297-303.
- [5] SINGH N K. Instability and transition in a laminar separation bubble[J]. *Journal of Applied Fluid Mechanics*, 2019, 12(5): 1511-1525.
- [6] DE SANTIS C, CATALANO P, TOGNACCINI R. Model for enhancing turbulent production in laminar separation bubbles[J]. *AIAA Journal*, 2022, 60(1): 473-487.
- [7] HORTON H P. Laminar separation bubbles in two and three dimensional incompressible flow[D]. London, UK: Queen Mary University of London, 1968.
- [8] WEIBUST E, BERTELROD A, RIDDER S O. Experimental investigation of laminar separation bubbles and comparison with theory[J]. *Journal of Aircraft*, 1987, 24(5): 291-297.
- [9] DE SANTIS C, CATALANO P, TOGNACCINI R. Model for enhancing turbulent production in laminar separation bubbles[J]. *AIAA Journal*, 2022, 60(1): 473-487.
- [10] ROBERTS L S, FINNIS M V, KNOWLES K. Forcing boundary-layer transition on a single-element wing in ground effect[J]. *Journal of Fluids Engineering*, 2017, 139(10): 101205.

**Acknowledgements** The Flight Measurement and Flow Control (FMFC) Innovation Laboratory at Nanjing University of Aeronautics and Astronautics provided experimental facility and instruments for this study. The following individuals are acknowledged by the authors for their assistance: GU Yunsong, ZHAO Dongkai, LIN Sihang, FANG Ruisihan, CHEN Yongqiang, SHI Nanxing and ZHANG Yuzhe.

**Authors** Mr. SIPKADUWA MADUWA GURUGE Supun Induwara Perera is presently pursuing an Engineering Master's degree in aerospace science and technology at Nanjing University of Aeronautics and Astronautics, and he obtained his Bachelor's degree in aeronautical engineering from the same university in 2023.

Dr. LI Linkai is presently an assistant professor in Nanjing University of Aeronautics and Astronautics. He received his Ph.D. degree in 2018 from Iowa State University (USA).

He also obtained his Master's and Bachelor's degrees in aerospace engineering from Nanjing University of Aeronautics and Astronautics in 2015 and 2012, respectively. His research interests include advanced flow diagnostics and instrumentation development, thermal-fluids physics, flow control and new concept aircraft design.

**Author contributions** Mr. SIPKADUWA MADUWA GURUGE Supun Induwara Perera prepared the model, conducted the experiment, collected the data and wrote the manuscript. Dr. LI Linkai designed the study, interpreted the results and wrote the manuscript. Mr. WANG Shilong contributed the experimental setup, data analysis, discussion and background of the study. All authors commented on the manuscript draft and approved the submission.

**Competing interests** The authors declare no competing interests.

(Production Editor: ZHANG Bei)

## 基于间歇扰动的NACA633-421翼型层流分离泡流动控制研究

SIPKADUWA MADUWA GURUGE Supun Induwara Perera,

李琳恺, 王世龙

(南京航空航天大学航空学院, 南京 210016, 中国)

**摘要:**研究了NACA 633-421翼型的气动性能,以及层流分离泡(Laminar separation bubble, LSB)间歇扰动流动控制方法的有效性和可行性。研究发现,合成射流激励器的平均速度和影响范围随驱动频率和驱动幅值的增加而增大。LSB会在 $Re=1.0\times 10^5$ 条件下形成,并且在 $\alpha=6^\circ$ 时发生破裂造成升力突降。但采用间歇扰动控制后,失速迎角(Angle of attack, AoA)增大,阻力明显减小。研究表明,虽然某些干扰幅值不能完全使机翼升力系数从LSB失速中恢复,但减小驱动幅值比增大合成射流驱动幅值更能部分恢复机翼气动性能,使得机翼的整体气动特性得以保持。

**关键词:**层流分离泡;间歇扰动控制;激励频率;驱动振幅;合成射流激励器